Published in final edited form as:
*Exp Dermatol*. 2011 January ; 20(1): 29–34. doi:10.1111/j.1600-0625.2010.01187.x.

# A novel biomarker harvesting nanotechnology identifies Bak as a candidate melanoma biomarker in serum

**Caterina Longo**[1,2,*], **Guido Gambara**[1,*], **Virginia Espina**[1], **Alessandra Luchini**[1], **Barney Bishop**[3], **Alexis S. Patanarut**[3], **Emanuel F. Petricoin III**[1], **Francesca Beretti**[4], **Barbara Ferrari**[2], **Enrico Garaci**[5], **Anto De Pol**[4], **Giovanni Pellacani**[2], and **Lance A. Liotta**[1]

[1]Center for Applied Proteomics and Molecular Medicine, George Mason University, Manassas, VA, USA

[2]Department of Dermatology and Venereology, University of Modena and Reggio Emilia, Modena, Italy

[3]Department of Chemistry and Biochemistry, George Mason University, Manassas, VA, USA

[4]Department of Anatomy and Histology and CIPro Proteomics Centre, University of Modena and Reggio Emilia, Modena, Italy

[5]Istituto Superiore di Sanità, viale Regina Elena, Rome, Italy

## Abstract

**Background—**Melanoma represents only 4% of all skin cancers, but nearly 80% of skin cancer deaths. This manuscript applies several new measurement technologies with the purpose of elucidating molecular signatures of melanoma aggressiveness.

**Purpose—**We sought to determine whether low-abundant serum proteins related to apoptotic pathways could be measured and correlated with defined melanoma subtypes. Hydrogel core shell nanoparticles, a new technology capable of selectively entrapping low molecular weight proteins and protecting them from enzymatic degradation, were used to capture candidate serum biomarkers. Biomarker levels were correlated with confocal microscopy, thereby representing a combination of new technologies for *in vivo* histologic documentation.

**Results—**Among a panel of analyzed serum proteins, Bak was differentially expressed between nevi and melanomas. Melanomas with higher Bak serum levels exhibited more pronounced junctional activity on confocal imaging, whereas lesions with ‘sparse’ dermal nests had weak Bak expression.

**Conclusions—**Our study links serum proteome analysis with confocal microscopic clinical *in vivo* histologic classification of melanomas. Bak has not been previously measured in serum. Bak

Correspondence: Caterina Longo, MD, PhD, Department of Dermatology, University of Modena and Reggio Emilia, via del Pozzo 71, 41124 Modena, Italy, Tel.: +39 (0)59 4224264, Fax: +39 (0)59 4224271, caterina.longo@unimore.it.
*These Authors equally contributed to the work.

**Conflict of interest**: The authors state no conflicts of interests.

Supporting Information
Additional Supporting Information may be found in the online version of this article:
Figure S1. Supervised Bayesian clustering of serum proteins harvested by nanoparticles.
Figure S2. Spearman's rho non-parametric analysis for determining protein associations.
Table S1. Endpoints analyzed by means of RPPMA.
Please note: Wiley-Blackwell are not responsible for the content or functionality of any supporting materials supplied by the authors. Any queries (other than missing material) should be directed to the corresponding author for the article.

differential expression among melanoma subtypes confirms the importance of the apoptotic pathway as a contributor to melanoma aggressiveness.

**Keywords**

biomarker; *in vivo* confocal microscopy; melanoma; nanotechnology; proteomics

## Introduction

Although the rates of cancer are stabilizing, the number of new melanomas continues to rise. Melanoma represents only 4% of all skin cancers, but nearly 80% of skin cancer deaths (1). Once melanoma spreads to regional and distant sites, the chance of cure decreases significantly. Unfortunately, current prognostic markers are often inadequate. The Breslow's thickness, measured from the top of the epidermal granular layer to the deepest invasive melanoma cell (2), remains the most powerful independent prognostic factor. However, it does not truly address the complexity and heterogeneity of individual melanoma subtypes that can lead to success of a targeted therapeutic agent. In fact, a minority of patients with thin melanomas will develop metastatic disease (3). The transformation from benign melanocytes to metastatic melanoma is the result of a compilation of genetic aberrations involving crucial cellular processes: cellular signaling network, cell cycle regulation, and cell death. Several marker molecules involved in these genetic alterations have been identified, and their expression in primary melanoma has been studied (4). BRAF mutations, with a special emphasis on the glutamic acid for valine substitution at the hotspot position 600 (V600E), and the concomitant activation of other signaling pathways have been investigated (5). A new interesting classification of melanoma different subtypes has been proposed by Curtin et al. and Viros et al. (6,7) It combines genetic aberrations with histomorphologic characteristics, resulting in new insights into the pathogenesis of this malignancy. Along with genetic profiling, the circulatory proteome has become one of the most promising molecular archives for the discovery of biomarkers in human diseases (8).

Discovery of new serum protein biomarkers useful for early diagnosis and prognosis of cancer is an urgent goal of the field of proteomics (9). Melanoma serum biomarkers are hindered by severe physiologic challenges: (i) the low abundance of serum biomarkers emanating from a small dermatologic lesion, (ii) the presence of high abundance proteins, such as albumin, that may interfere with the detection of low-abundant biomarkers, and (iii) degradation of the protein postcollection (8). A new class ‘smart’ nanoparticles have been created to overcome these physiologic challenges. In this study, we employed core shell, bait-loaded nanoparticles that are capable of selectively entrapping low- abundance and molecular weight target analytes and protecting them from enzymatic degradation (10–12). We used the nanoparticles to harvest serum proteins from patients with atypical nevi, melanoma. To measure the candidate low-abundance serum biomarkers with high sensitivity, the biomarkers captured by the nanoparticles were measured by another new technology: the reverse-phase protein microarray (RPMA) platform (13). This combination of technologies permitted the successful measurement of activated signal pathway molecules that exist at extraordinary low concentrations in serum. We focused on apoptosis-related proteins because of the important role of apoptosis for the growth regulation of neoplasms and particularly melanoma (14,15). A third unique clinical research application applied in this study was *in vivo* reflectance-mode confocal microscopy (RCM) (16,17). RCM was employed to morphologically characterize all melanocytic lesions before surgical excision and serum collection. The combination of smart nanoparticles, RPMA and confocal microscopy provides clinicians with the opportunity to correlate relevant morphologic aspects of melanocytic lesions with low-abundance serum biomarker profiles.

In this report, we analyzed apoptotic pathway serum proteins from patients with benign nevi and melanoma combined with the lesion's *in vivo* morphologic aspects as an initial step in understanding the protein signature of individual melanoma subtypes in relation to their heterogeneous clinical and biologic behavior.

## Methods

### Patient samples

Fifty-five sera were prospectively collected before surgical excision, at the University of Modena and Reggio Emilia, Department of Dermatology, Modena, Italy under IRB approval (protocol number 1338/CE) with informed patient consent. The study population consisted of patients with melanocytic lesions excised following the standard of care dermoscopic criteria for melanoma. All excised lesions were considered 'atypical' upon clinical and dermoscopic examination. Lesions located on suitable sites were further characterized by *in vivo* confocal microscopy. All cases were matched for sex and age (±5 years). Sera were frozen in 600 $\mu$l aliquots at −80°C without any additives. Smart nanoparticles were incubated with serum samples, and the particle eluates were analyzed by RPMA. Histopathologic report was obtained. Melanoma thickness according to Breslow was considered. Nevi were classified into junctional, compound or intradermal, and the presence of dysplasia (moderate to severe) was reported.

### Confocal microscopy image acquisition

The RCM images were acquired by a near-infrared reflectance confocal laser scanning microscope (Vivascope 1500®; Lucid Inc., Henrietta, NY, USA). This system employs a diode laser at a wavelength of 830 nm and a 30× water immersion objective lens with numeric aperture of 0.9 (18). A sequence of single confocal images and a sequence of montages of single high-resolution images (500 × 500 $\mu$m), called 'Vivacube', were acquired, at the level of the epidermis, basal layer/dermo-epidermal junction, and superficial dermis, respectively (19). RCM features for 17 melanoma cases were described considering two major relevant confocal criteria (Fig. 1).

**Cytology—**This denotes the presence of atypical melanocytic cells within the epidermis, distinguishing between (i) cells spreading upwards in a pagetoid fashion and (ii) cells located at basal layer level. (20).

**Architecture—**(i) This denotes presence of junctional nests, giving rise to a 'mesh-work pattern' that is represented by a predominance of junctional thickenings corresponding to enlargements of interpapillary space formed by aggregated cells and/or clusters bulging within dermal papilla in contiguity with basal layer; and (ii) the presence of dermal nests, defined as 'dense' dermal nests or 'sparse' dermal nests (roundish non-reflecting structures with a well-demarcated border, containing bright nucleated cells), corresponding on histology to homogeneous or dishomogeneous clusters, respectively (16).

### Core-shell particle synthesis and characterization

Core-shell hydrogel nanoparticles were synthesized and characterized as previously described (10,11,21). Briefly, the particle architecture used in our study has a NIPAm shell that surrounds a N-isopropylacrylamide-acrylic acid core (NIPAm/AAc core), containing affinity bait moieties. The sieving capability of the NIPAm shell shields the core and its affinity bait groups from larger molecules that may be present and could compete with the intended low-abundance, low molecular weight molecular targets for binding to the affinity bait in the core. Light scattering characterization of the particles showed that the core diameter at 25°C and pH 4.5 was 364.7 ±4.3 nm whereas the diameter of the core–shell

particles at the same conditions was 699.4 ± 6.2 nm. Nanoparticles were further characterized by means of atomic force microscopy to confirm size homogeneity. Nanoparticles concentration, as obtained by weighing the lyophilized particles, was 10 mg $ml^{-1}$, and the number of particles per mL was 230 millions.

### Protein extraction/elution

A volume of 30 $\mu$l of 4× Laemmli Buffer was added to the nanoparticle pellet, and the sample was boiled on a heating block at 100°C for 8 min. Samples were centrifuged (7 min, 25°C at 16.1 rcf), and the supernatant (nanoparticle elution) was saved and stored at −20°C before use. Prior to serial dilutions, samples were initially diluted 1:2 using a lysis buffer consisting of equal volumes of T-PER® (Pierce, Rockford, IL, USA) and 2× Tris-glycine-SDS sample buffer (Invitrogen, Carlsbad, CA, USA) in the presence of 10% of TCEP (Thermo Fisher Scientific Inc., Waltham, MA, USA). The samples were heated on a heating block at 100°C for 5 min.

### Construction of reverse-phase protein microarrays (RPMA)

The nanoparticle eluates and control cell lysates were printed in duplicate on glass-backed nitrocellulose array slides (FAST slides; Whatman, Florham Park, NJ, USA) as previously described (22). Approximately, 30 nl of each sample was printed in a dilution curve representing neat, 1:2, 1:4 and 1:8 dilutions.

### Immunostaining and analysis of reverse-phase protein microarrays

RPMAs were blocked with PBS supplemented with 0.2% I-Block (Applied Biosystems/Tropix) and 0.1% Tween 20 at least for 1 h with constant rocking at room temperature. RPMAs were stained as previously described (13) with an Autostainer (Dako, Carpinteria, CA, USA) following manufacturer directions using a catalyzed signal amplification system (Catalyzed Signal Amplification System; Dako). All antibodies were subjected to extensive validation for single band, appropriate MW specificity by Western blot (23). Stained arrays were scanned on a UMAX Powerlook1120 flatbed scanner (UMAX, Dallas, TX, USA). Total protein content of each array spot was detected using Sypro Ruby Protein Blot Stain (Invitrogen) by a CCD-equipped scanner (NovaRay; Alpha Innotech, San Leandro, CA, USA). The intensity of each spot was digitized using Image-Quant version 5.2 (GE Healthcare, Piscataway, NJ, USA).

### Immunohistochemical staining of tissue sections (IHC)

Four-micrometer paraffin embedded sections were cut, mounted on adhesive-coated slides, and dried at 60°C for 30 min. IHC was performed according to manufactures' instructions. The slides were incubated with an antibody to Bak (1:500; Epitomics Inc., Burlingame, CA, USA). Negative controls were included by omitting Bak antibody during the primary incubation. Two compartments were considered: Bak positivity within the epidermis and Bak positivity into the dermis (nests or single melanocytic cells).

### Statistical methods

Median and interquartile ranges were calculated for patient's age and melanoma Breslow's thickness.

Reverse-phase microarray data were quantified by ImageQuant software, and statistical analysis was performed with Excel, JMP, and R statistical software. RPMA data were presented as the mean ± SEM. Student's *t*-test was used for statistical comparison between means where applicable. Statistical evaluation was carried out employing the SPSS statistical package (release 12.0.0, 2003; SPSS Inc., Chicago, IL, USA).

Non-parametric Spearman rho correlations between RPMA measured proteins and melanoma thickness were calculated (JMP ver5.2, SAS Institute Inc., Cary, NC, USA). Multivariate discriminant analysis was employed to determine independently significant proteins to predict melanoma diagnosis and to differentiate between thin and thick melanomas.

Relative and absolute frequencies of confocal features and immunohistochemistry patterns were evaluated in melanoma cases. Confocal features in melanomas, immunohistochemistry patterns, and their correlation with independently significant serum proteins were calculated with Spearman's rho test. Chisquare test of independence (Fisher's exact test was applied if any expected cell value in the 2 × 2 table was <5) was used to compare melanoma confocal and immunohistochemistry aspects with different Bak serum level.

## Results

### Patient samples and clinical characteristics

The study population consisted of 29 serum samples from primary and metastatic melanoma (median age of 49.3 years, 37.8–58.3 interquartile range) and 26 serum samples from patients with atypical melanocytic nevi (median age of 54.5 years, 43.6–61.7 interquartile range). All sera were collected at University of Modena and Reggio Emilia, Italy under IRB approval with informed consent. Melanomas had a mean Breslow's thickness of 0.63 mm, 0.37–1.6 interquartile range. No *in situ* melanomas were reported; sixteen melanomas were equal or less than 1 mm (T1 staging according to AJCC) (24,25), five were between 1.01 and 2 mm (T2), four between 2.01 and 4 mm (T3), one thicker than 4 mm, and three in transit metastasis. Atypical melanocytic nevi comprised six junctional nevi, eighteen compound nevi, and two intradermal nevi. Considering the presence of histologic dysplasia, fourteen nevi showed moderate to severe dysplasia.

To identify candidate biomarkers involved in the early stage or progression of melanoma, serum collected from 29 patients with melanoma at different stages and from 26 individuals with atypical nevi was incubated with ‘smart’ hydrogel nanoparticles (10,11). The nanoparticles sequestered low-abundance protein that was eluted for analysis by RPMA. A total of 24 signaling proteins were analyzed by RPMA. Each array was stained using antibodies against 18 phospho-proteins and other six signaling proteins (Table S1). All 24 proteins were detected in the sera of patients with melanoma and individuals with atypical nevi. Example proteins are shown in Fig. S1. This is the first evidence that phosphoproteins can be detected in serum following a new workflow that includes the enrichment of low-abundance proteins by means of serum preprocessing with NIPAm/AAc nanoparticles and subsequent analysis by RPMA.

Among the several endpoints, serum prosurvival cell signaling pathway proteins such as PDGF-BB, mTOR Ser2481, Cleaved Caspase 9 Asp315, and Bcl2 have been identified and reliably measured by RPMA from NIPAm/AAc nanoparticle processed samples. Moreover, detection and measurement of PDGF-BB, which has been previously found to contribute to tumor neo- angiogenesis in melanoma, demonstrated the validity of the method. In fact, it is a very labile, low molecular weight protein present in serum at extremely low concentration (26).

Serum PDGF-BB values were significantly correlated with serum mTOR Ser2481 values in patients with melanomas thicker than 1 mm. Conversely, serum Bcl2 values were significantly correlated with Cleaved Caspase 9 Asp315 in patients with thin melanomas (Fig. S2).

Considering the whole population (nevi and melanomas), no statistically significant differences were found among the analyzed endpoints. No differences were also observed considering nevus type (junctional, compound, intradermal). However, a pro-apoptotic protein named Bak has been found as a candidate serum biomarker.

### Bak is differently abundant in serum from patients with dysplastic nevi

Distinguishing the nevus population for the presence of moderate to severe histologic dysplasia, Bak showed higher value in the group of dysplastic nevi (mean ± SD = 4.87 ± 1.55) compared to non-dysplastic lesions (mean ± SD = 3.62 ± 1.74) ($P = 0.064$).

### Bak is differentially abundant in serum from melanoma patients with different Breslow's thickness

To investigate the potential prognostic value of signaling proteins in serum, we compared sera of patients with melanoma with a Breslow thickness <1 mm with sera of patients with a Breslow thickness >1 mm. Among the 24 endpoints analyzed, Bak was significantly lower ($P < 0.03$) in the sera collected from patients with a Breslow thickness >1 mm (mean ± SD = 3.68 ± 1.32) compared with patients with a Breslow thickness <1 mm (mean ± SD = 4.71 ± 1.89) (Fig. 2).

Interestingly, the three melanoma metastasis showed the lowest Bak value (mean ± SD = 2.65 ± 0.38). A receiver operating characteristic curve with an area under the curve of 0.70 (95% confidence interval = 0.51–0.91) was obtained. The Bak value equal or greater than 4.38 represented the most accurate threshold to discriminate between thin and thick melanomas with an overall diagnostic accuracy of 74.3%. These results suggest that Bak may be a new candidate serum melanoma biomarker that could improve the risk stratification of patients with melanoma, and the above-mentioned threshold can represent the cutoff level to consider high or low profiling of Bak. In fact, thin melanomas (56.3%) and dysplastic nevi (57.1%) showed serum Bak level higher than the threshold compared to thick melanomas and metastasis (7.6%) and non-dysplastic nevi (20%).

### Correlation between Bak serum levels and *in vivo* melanoma imaging aspects

Bak serum levels measured by RPMA were correlated with previously identified relevant confocal parameters (16). Within the evaluated confocal parameters, the presence of junctional nests and the absence of sparse dermal nests correlated with high relative Bak serum levels. It is notable that all lesions showing junctional nests exclusively (and not dermal nests) were characterized by high Bak serum level whereas melanomas presenting sparse dermal nests on confocal images (in the absence of junctional nests) had low levels of serum Bak. The presence of both junctional and dermal nests, as well as the absence of them, was not predictive of Bak serum levels.

No statistical significant differences were found in relation with cytologic aspects of melanomas as evaluated by RCM. A border line $P$ value ($P = 0.086$) was found for melanomas showing high Bak serum level and the collateral presence of dendritic-shaped pagetoid cells and atypical melanocytes at the basal layer.

### Correlation of Bak serum levels with IHC

Immunohistochemistry was performed on 13 melanoma cases. Positive IHC Bak scores (semiquantitative scoring) were compared to Bak serum levels. Bak serum levels were significantly correlated with the presence of Bak in the epidermis (Spearman's rho 0.556, $P = 0.048$). All cases with high Bak serum levels showed epidermal positivity for Bak (Fig. 3), five of which were strongly positive. In contrast, cases with low Bak serum levels, only one

case showed marked epidermal positivity for Bak and two cases exhibited weak immunoreactions; the remaining two cases were completely negative.

## Discussion

Melanoma is the most devastating form of skin cancer and represents a leading cause of cancer death, particularly in young adults (1,27). Current morphological and histological criteria (anatomic site and type of the primary tumor, tumor size and invasion depth, ulceration, vascular invasion, and mitotic index) cannot truly address the complexity and heterogeneity of melanoma in relation to its unpredictable biologic behavior and prognosis. The emerging scenario on the molecular complexity in melanoma tumors mirrors the clinical variety of the disease and highlights the concept that melanoma is not a single disease but a heterogeneous group of disorders that involve complex molecular changes. In light of the new discoveries on melanoma biology, the efforts have been directed to link the molecular aberrations (genetic or signaling pathways) with clinical and morphologic aspects among the melanoma tumors (6,7).

The circulating proteome is thought to be a rich source of relevant biomolecules (low-abundance circulating proteins and peptides) which can provide information regarding the state of the organism as a whole (8). In the present study, we interrogate serum samples belonging from patients with melanoma and atypical nevi, for the presence of relevant proteins or fragments. The availability of harvesting nanoparticle combined with the RPMA technology now makes it possible to discover and measure low abundance biomarkers that could not be detected in the past because they exist below the sensitivity of conventional assay methods. We present the first evidence that phospho-proteins can be detected in serum following a new workflow that includes enrichment of low-abundance proteins by means of serum preprocessing with hydrogel nanoparticles, with subsequent analysis by RPMA (11). It has been previously shown that core-shell nanoparticles composed of NIPAm/AAc and a shell of N-isopropyl-acrylamide were able to concentrate PDGF-BB and other low abundant and short half-life chemokines (11). Moreover, Luchini et al. (10) demonstrated that NIPAm/AAc nanoparticles were suitable for capturing and concentrating low-abundance biomarkers from serum for proteomic analysis. The present study details the use of a new workflow that combines the preprocessing of sera with ‘smart’ hydrogel nanoparticles with analysis by RPMA to identify low-abundance candidate serum biomarkers. Among the endpoints probed by RPMA, Bak emerged as a relevant protein. It is a pro-apoptotic protein involved in the intrinsic pathway that is regulated by Bcl-2 family proteins, and it is usually activated by cytotoxic events (28). The Bcl-2 family is composed of three classes of proteins: apoptosis inhibitors (such as Bcl-2, Bcl-XL, Bcl-W, Mcl1, and Bcl-B), pro-apoptotic proteins (Bax, Bak and Bok), and a third class that can regulate the activity of anti-apoptotic Bcl-2 proteins to induce apoptosis (Bad, Bid, Hrk, BIM, Bmf, NOXA and PUMA). Pro-apoptotic Bax and Bak promote the release of cytochrome c or diablo from mitochondria leading to caspase activation (29). On the other side, the anti-apoptotic Bcl-2 family proteins, such as Bcl-2 and Bcl-XL, inhibit Bax and Bak (30,31). Downregulation of apoptotic pathways that promote the survival of melanoma cells has been previously reported. The intrinsic apoptosis resistance of melanoma cells has been shown to occur through over expression of pro-apoptotic proteins (32–35). The role of Bak as a negative prognostic factor (33) as well as its relevance in cisplatin-induced apoptosis has been reported (36). Fecker et al. found in their study that loss of expression of the pro-apoptotic Bcl-2 family members Bax and Bak was significantly correlated with prognosis in superficial spreading melanoma type, even though the patients did not significantly differ in age or Breslow tumor thickness. Moreover, tumors that had lost both Bax and Bak expression were found exclusively in the group of superficial spreading melanoma with progression, suggesting that, at least in those melanomas, a Bax/Bak-controlled pathway

needs to be operative to prevent tumor progression. Similarly, we found that Bak was a relevant protein to discriminate between thin and thick melanomas. The novelty of our work consists in the discovery of Bak in serum and not only on paraffin embedded tissues. Although no prognostic data have been considered in our study set, Bak was differently expressed in melanoma presenting different cyto-architectural aspects detected *in vivo* by RCM.

Interestingly, the presence of high Bak serum levels was strongly correlated in melanoma containing junctional nests on confocal *in vivo* evaluation. These melanomas were traditionally classified as superficial spreading type. Among superficial spreading types, melanomas with junctional activity showed strong Bak positive immunoreactions in respect of those not having junctional nests.

Conversely, melanomas characterized by dermal nests, sparse type, and by few to absent junctional activity possessed low-Bak serum levels. To our knowledge, no previous research studies have had the capability to link serum protein biomarker data with *in vivo* melanoma morphologies by means of dynamic RCM. The relevance of Bak expression in relation to melanoma morphologies holds the potential to understand the heterogeneous biologic lesions with high growth rate compared to others with indolent behavior.

The relationship between reflectance confocal microscopy and serum Bak levels was confirmed by IHC that showed a strong positive Bak immunoreactions for melanocytes located at dermoepidermal junction and into the epidermis whereas a weak Bak immunoreactivity was noted in the cytoplasm of cells in dermal nests. It has to be emphasized that no *in situ* melanomas were included in our study population. This means that Bak is a potential novel melanoma biomarker that can discriminate melanomas along a continuum of Breslow's thickness, on the basis of slight morphologic differences. Interestingly, atypical melanocytic nevi with moderate-to-severe dysplasia showed a high Bak level, similarly to melanoma characterized by junctional activity. This opens the never ending question of the possibility of transformation of these lesions into malignancy and in their subsequent correct classification.

While the data presented in this report represent a small study set, the cases were supported by detailed clinical data, were age matched, and were characterized by *in vivo* histologic documentation. Based on the present findings, serum apoptosis markers should be validated in a larger tumor data set and correlated with long-term prognosis and follow-up.

In conclusion, our data underline the critical role of the mitochondrial pathway for apoptosis signaling in primary melanoma and the role of Bak as a candidate serum biomarker. The weak serum value of Bak appears to be characteristic for tumor progression being present in tumors with dermal nesting and not longer presenting junctional activity. Defining an individual patient's unique tumor characteristics by means of new *in vivo* imaging such as RCM and linking them with laboratory findings may lead to a better understanding of the tumor signature as a whole in a translational effort from the bench to the bedside.

## Supplementary Material

Refer to Web version on PubMed Central for supplementary material.

## Acknowledgments

This work was partly supported by the Italian Istituto Superiore di Sanità, Rome, Italy in the framework of the Italy/USA cooperation agreement between the U.S. Department of Health and Human Services, George Mason University and the Italian Ministry of Public Health. This work was partially supported by the U.S. Department of

Energy grant number DE- FC52-04NA25455. University of Modena was partly supported by a grant of the Istituto Superiore di Sanità, Rome, Italy, (Project nr. 527/B/3A/4).

## References

1. Jemal A, Siegel R, Ward E, et al. CA Cancer J Clin. 2008; 58:71–96. [PubMed: 18287387]
2. Breslow A. Ann Surg. 1970; 172:902–908. [PubMed: 5477666]
3. Becker D, Mihm MC, Hewitt SM, et al. Cancer Res. 2006; 66:10652–10657. [PubMed: 17108101]
4. Braun-Falco M, Schempp W, Weyers W. Exp Dermatol. 2009; 18:12–23. [PubMed: 19054055]
5. Dankort D, Curley DP, Cartlidge RA, et al. Nat Genet. 2009; 41:544–552. [PubMed: 19282848]
6. Curtin JA, Fridlyand J, Kageshita T, et al. N Engl J Med. 2005; 353:2135–2147. [PubMed: 16291983]
7. Viros A, Fridlyand J, Bauer J, et al. PLoS Med. 2008; 5:e120. [PubMed: 18532874]
8. Liotta LA, Ferrari M, Petricoin E. Nature. 2003; 425:905. [PubMed: 14586448]
9. Ugurel S, Utikal J, Becker JC. Cancer Control. 2009; 16:219–224. [PubMed: 19556961]
10. Luchini A, Geho DH, Bishop B, et al. Nano Lett. 2008; 8:350–361. [PubMed: 18076201]
11. Longo C, Patanarut A, George T, et al. PLoS ONE. 2009; 4:e4763. [PubMed: 19274087]
12. Fredolini C, Meani F, Reeder KA, et al. Nano Res. 2008; 1:502–518. [PubMed: 20467576]
13. Espina V, Mehta AI, Winters ME, et al. Proteomics. 2003; 3:2091–2100. [PubMed: 14595807]
14. Cory S, Adams JM. Nat Rev Cancer. 2002; 2:647–656. [PubMed: 12209154]
15. Tchernev G, Orfanos CE. J Cutan Pathol. 2007; 34:247–256. [PubMed: 17302609]
16. Pellacani G, Guitera P, Longo C, et al. J Invest Dermatol. 2007; 127:2759–2765. [PubMed: 17657243]
17. Guitera P, Pellacani G, Longo C, et al. J Invest Dermatol. 2009; 129:131–138. [PubMed: 18633444]
18. Rajadhyaksha M, Grossman M, Esterowitz D, et al. J Invest Dermatol. 1995; 104:946–952. [PubMed: 7769264]
19. Pellacani G, Cesinaro AM, Longo C, et al. Arch Dermatol. 2005; 141:147–154. [PubMed: 15724010]
20. Pellacani G, Cesinaro AM, Seidenari S. J Invest Dermatol. 2005; 125:532–537. [PubMed: 16117795]
21. Luchini A, Longo C, Espina V, et al. J Mater Chem. 2009; 19:5071–5077. [PubMed: 20585471]
22. VanMeter AJ, Rodriguez AS, Bowman ED, et al. Mol Cell Proteomics. 2008; 7:1902–1924. [PubMed: 18687633]
23. Paweletz CP, Charboneau L, Bichsel VE, et al. Oncogene. 2001; 20:1981–1989. [PubMed: 11360182]
24. Balch CM, Buzaid AC, Soong SJ, et al. J Clin Oncol. 2001; 19:3635–3648. [PubMed: 11504745]
25. Balch CM, Gershenwald JE, Soong SJ, et al. J Clin Oncol. 2009; 27:6199–6206. [PubMed: 19917835]
26. Barnhill RL, Xiao M, Graves D, et al. Br J Dermatol. 1996; 135:898–904. [PubMed: 8977709]
27. Pellacani G, Lo Scocco G, Vinceti M, et al. J Eur Acad Dermatol Venereol. 2008; 22:213–218. [PubMed: 18211415]
28. Kang MH, Reynolds CP. Clin Cancer Res. 2009; 15:1126–1132. [PubMed: 19228717]
29. Degli Esposti M, Dive C. Biochem Biophys Res Commun. 2003; 304:455–461. [PubMed: 12729579]
30. Youle RJ, Strasser A. Nat Rev Mol Cell Biol. 2008; 9:47–59. [PubMed: 18097445]
31. Vaux DL, Cory S, Adams JM. Nature. 1988; 335:440–442. [PubMed: 3262202]
32. Eberle J, Fecker LF, Hossini AM, et al. Oncogene. 2003; 22:9131–9141. [PubMed: 14668794]
33. Fecker LF, Geilen CC, Tchernev G, et al. J Invest Dermatol. 2006; 126:1366–1371. [PubMed: 16528364]
34. Kirkin V, Joos S, Zornig M. Biochim Biophys Acta. 2004; 1644:229–249. [PubMed: 14996506]

35. Daniel PT, Schulze-Osthoff K, Belka C, et al. Essays Biochem. 2003; 39:73–88. [PubMed: 14585075]
36. Mandic A, Viktorsson K, Molin M, et al. Mol Cell Biol. 2001; 21:3684–3691. [PubMed: 11340162]

## Abbreviations

| | |
|---|---|
| **RPMA** | Reverse-Phase Microarray |
| **RCM** | Reflectance Confocal Microscopy |
| **IHC** | immunohistochemistry |
| **PDGF-BB** | Platelet- Derived Growth Factor-BB |
| **NIPAm/AAc** | N-isopropylacrylamide-acrylic acid core |

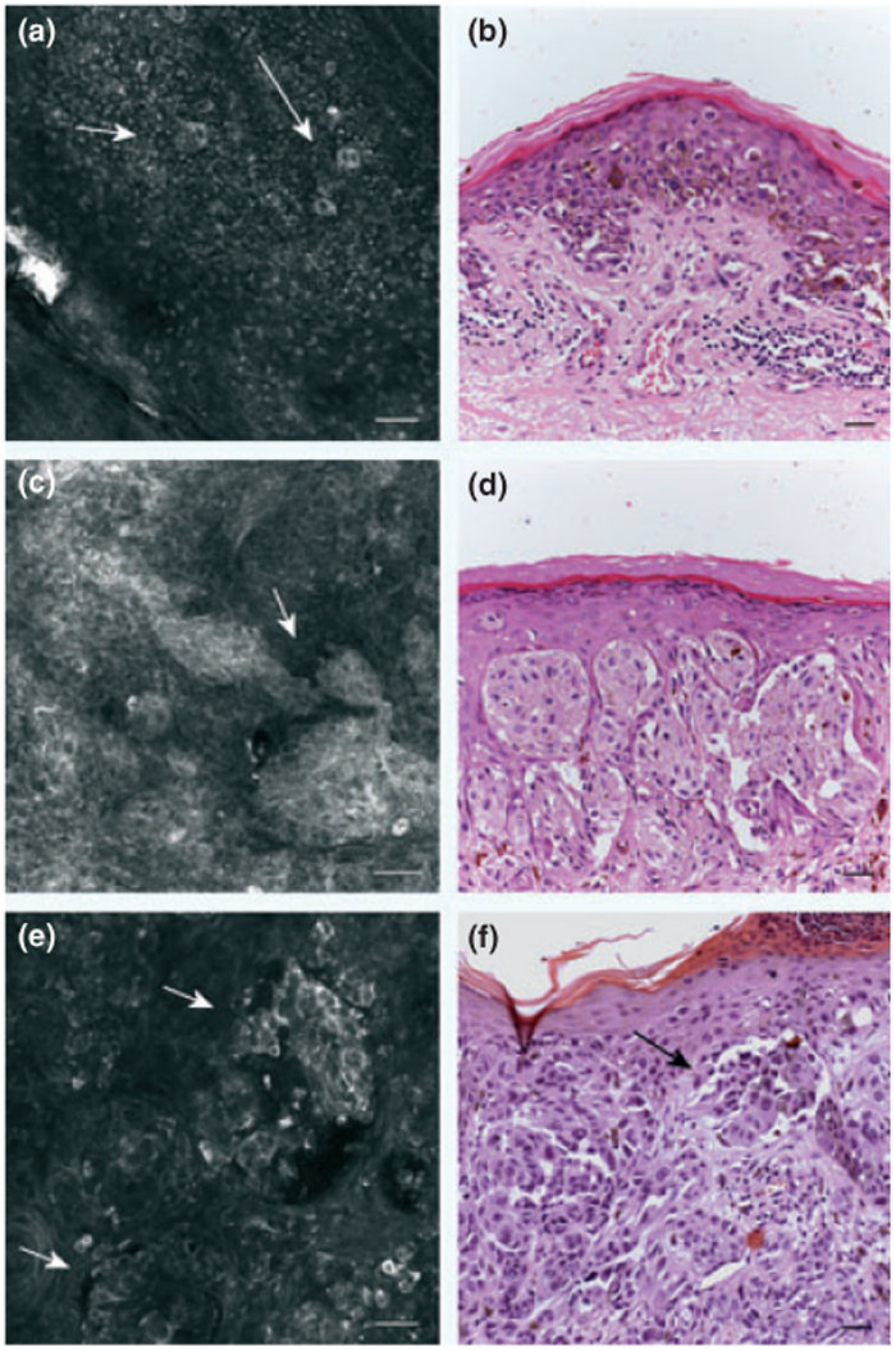


**Figure 1.**
Confocal images of melanoma. (a) confocal image (500 × 500 μm) at epidermal level showing the presence of roundish pagetoid cells (arrows). (b) H&E stained section (bar = 50 μm). Original magnification 20×. Abundant pagetoid cells in a melanoma. (c) confocal image (500 × 500 μm) at dermo-epidermal junction: junctional nests showing single atypical cells and in contiguity with basal layer. (d) H&E stained section (bar = 50 μm). Original magnification 20× presence of junctional atypical clusters in a melanoma. (e) confocal image (500 × 500 μm) at dermal level: sparse nests (f) H&E stained section (bar = 50 μm). Original magnification 20×. Corresponding melanocytic proliferation forming discohesive nests in an invasive melanoma.

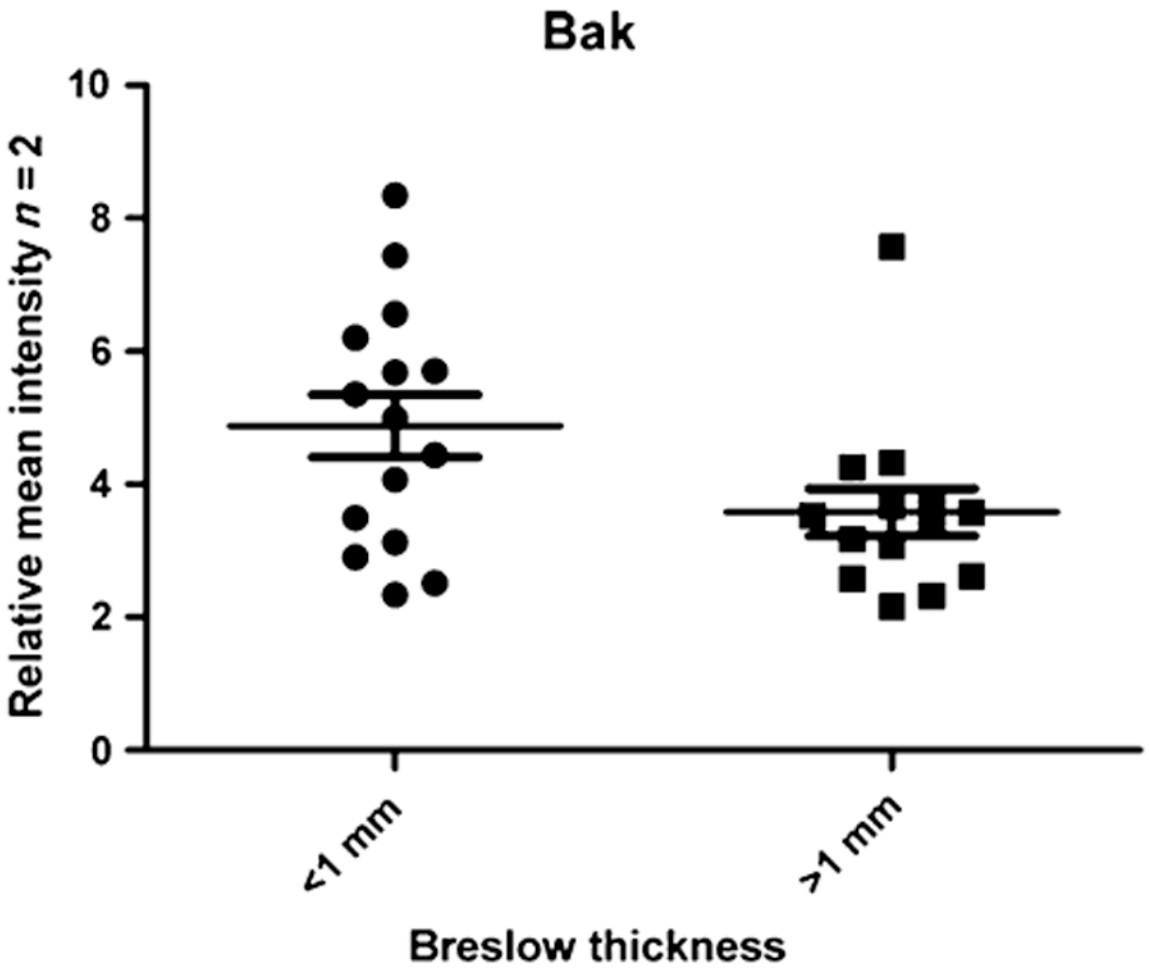


**Figure 2.**

Serum pro-apoptotic protein Bak discriminates melanocytic lesions based on Breslow's thickness. Scatterplot of the relative intensity of Bak measured by RPMA in sera collected from patients with a Breslow thickness <1 mm compared with patients with a Breslow thickness >1 mm. The level of Bak was significantly lower ($P < 0.03$) in the latter group.

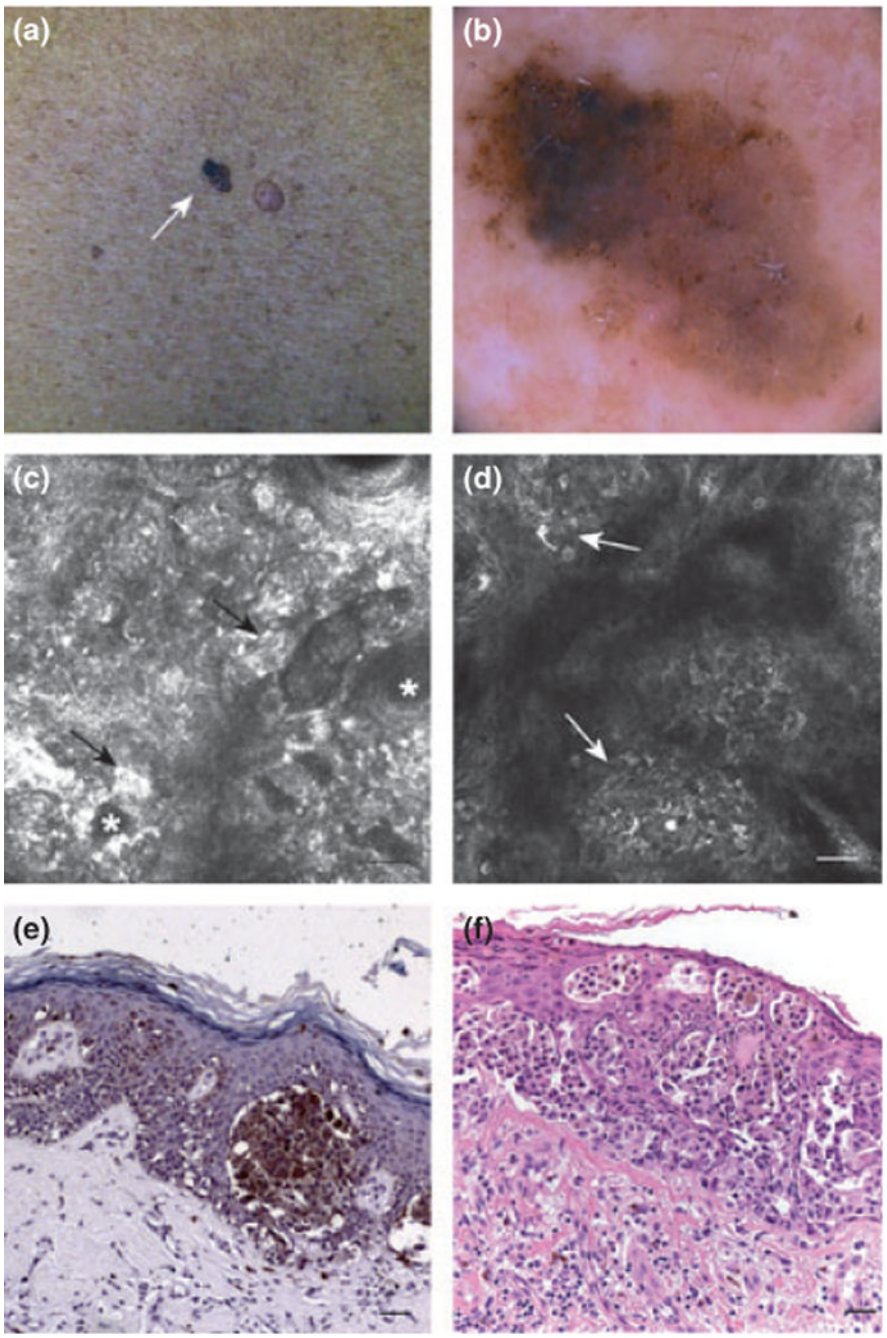


**Figure 3.**

Clinical images of melanoma. (a) Clinical picture of a melanoma (*arrow*). (b) Dermoscopic image suggestive of melanoma diagnosis (c) confocal image (500 × 500 $\mu$m) at basal layer: atypical junction refractive nests (*arrows*) around dermal papillae (*asterisks*). (d) confocal image (500 × 500 $\mu$m) at epidermal level: atypical pagetoid cells with dendritic branches admixed with roundish bright melanocytes (*arrows*) in a context of disrupted epidermal pattern. (e) IHC for Bak protein. Original magnification 20× (bar = 50 $\mu$m). Bak protein was shown immunohistochemically as granular brown cytoplasmic staining in the malignant melanocytes predominantly arranged in junctional nests and in single pagetoid cells. (f) H&E stained section (bar = 50 $\mu$m). Original magnification 20×. melanoma presenting a

marked pagetoid scattering of large epitheliod cells, occupying the entire epidermis and forming junctional clusters.